Characterize the magnetic signal generated in the magnetosphere from geomagnetic observations from 1999 to 2024

Yalei Shi, Vincent Lesur, Erwan Thébault

Characterize the magnetic signal generated in the magnetosphere from geomagnetic observations from 1999 to 2024

Yalei SHI[1], Vincent LESUR[1], Erwan THEBAULT[2]

[1]Université Paris Cité, Institut de physique du globe de Paris, CNRS F-75005 Paris, France
[2]Université Clermont-Auvergne, Laboratoire Magmas et Volcans, CNRS F-63170 Aubière, France

EUROPEAN SPACE WEATHER WEEK 2024

Introduction

In the near-Earth geomagnetic field region (Langel et al. [1996]), the main contribution to the geomagnetic field is from the core, but fields generated from the magnetosphere during magnetic storms may have geomagnetic field contributions up to hundreds of nanoteslas (nT). A challenging task is to separate the magnetospheric fields from other contributing sources of internal and external origin. Magnetic field measurements are available at different altitudes, from the surface to the orbits of the Low Earth Orbiting satellites. Magnetic survey satellite data provide an homogeneous spatial resolution but their spatiotemporal resolution is coarse thus limiting our ability to study rapidly varying external magnetic fields (CC. Finaly et al. [2017]). In contrast, ground geomagnetic observatories provide datasets with high temporal resolution of an hour over a large range of latitudes and longitudes that are particularly well suited to characterize magnetospheric signals. We describe here an approach to modeling the magnetospheric signal by replying on a Kalman filter approach (Kalman [1960]) and correlation-based technique (Holshneider et al. [2016]). We use hourly averaged magnetic field triplet measurements at the location of 218 magnetic observatories (see Figure 1) during geomagnetically quiet time. We then derive a time series of model coefficients describing the external field and its induced response in the Earth's interior and compare their time variations with the magnetospheric ring current index (RC), a magnetic proxy determined by other methodologies (Leonie et al. [2017]). The correlation between our axial dipole spherical harmonic coefficient (q10) and the external RC index is 0.9. Semi-annual, monthly, and daily variations, as well as tidal variations, are highlighted in the temporal spectra domain of magnetospheric gauss coefficients. A key element of our approach is ensuring that all model parameters are accompanied by robust error estimates.

Objective:

- Study the magnetospheric field up to spherical harmonic (SH) degree 6 (L=6) over 26 years from 1999 to 2024 covered 2 solar cycles through normal distributions ($\mathcal{N}(\mu = \mathrm{m}, \sigma^2 = C_m)$) with a time resolution of an hour, based on a Kalman filter and correlation-based technique.

INTERMAGNET observatory data

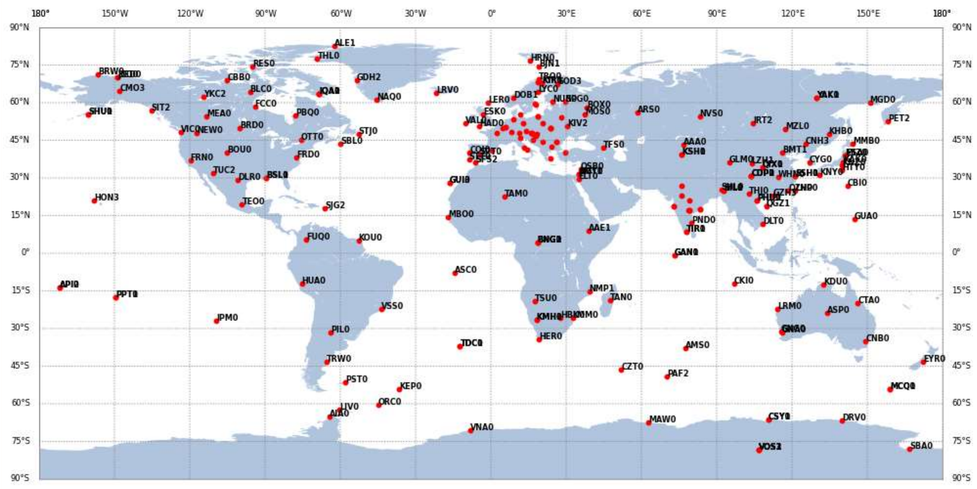

1, The main magnetic field contribution is removed from the hourly-mean INTERMAGNET observatory data over 26 years from 1999 to 2024 by subtracting the MCM model (Ropp et Lesur [2020])

2, Observatory data are selected during geomagnetically quiet time (Dst between -30 nT and 30 nT) and cleaned for outliers.

Figure 1: Distribution of the 218 geomagnetic observatory positions over 26 years

Parameters

The geomagnetic vector components after the selection are modeled in terms of spherical harmonics with the sum of the magnetospheric fields, induced fields, crustal offsets and ionospheric statistical contribution at each observatory location:

$$B(r,,\phi) = \sum_{\ell,m} q_\ell^m (\frac{r}{a})^{\ell-1} Y_\ell^m(\theta,\phi) + \sum_{\ell,m} i_\ell^m (\frac{a}{r})^{\ell+2} Y_\ell^m(\theta,\phi) + \sum_{i\in N_{obs}} \delta(r-r_i,\theta-\theta_i,\phi-\phi_i) O_i + \sum_{i\in N_{obs}} \delta(r-r_i,\theta-\theta_i,\phi-\phi_i) Io_i$$

	magnetosphere	induced field	crustal offset	Ionosphere
Coef.	q_ℓ^m	i_ℓ^m	O_i=(O_x^i, O_y^i, O_z^i)	Io_i=(Io_x^i, Io_y^i, Io_z^i)
m_0	$q_{l=1}^m \neq 0, q_{l>1}^m = 0$	0	O_i	Io_i (Astrid [2017])
C_0	V_ℓ^{ext}=$R(\ell)$=$S(\frac{R}{a})^{2\ell}$	$0.3^2 V_\ell^{ext}$ (Maus et al. [2005])	V_o	V_{Io} (Astrid [2017])
S	$0.7.10^4(nT^2)$ (Maus et al. [2005])	-	-	-
R	$3.5.10^4$km (Maus et al. [2005])	-	-	-
τ,($P = e^{-\frac{\Delta t}{\tau}}$)	10 hr (Hnat B. [2019])	10 hr	10^6 year (Ropp, Lesur [2020])	24 hr
A	$\sum_{\ell,m}(\frac{r}{a})^{\ell-1} Y_\ell^m$	$\sum_{\ell,m}(\frac{a}{r})^{\ell+2} Y_\ell^m$	1	1
Nb. of par.	48	48	3×218	3×218

Approach -- Kalman Filter

- **Prior information:**
  mean prior model m_0, prior covariance matrix C_0 as theoretical statistical prior information
- **Analysis step:**
  adjustment of models at the ***k***th hour by fitting INTERMAGNET observatory data, based on the Least Squares method

$$d = Am + \mathrm{e}$$
$$m_k^* = m_k + (A^t C_e^{-1} A + C_k^{-1})^{-1} A^t C_e^{-1} (d - Am_k)$$
$$C_k^* = (A^t C_e^{-1} A + C_k^{-1})^{-1}$$

- **Prediction step:**
  prediction of the next hour's model (at the ***(k+1)***th hour) from the adjusted model at the step ***k*** and based on a prediction operator P

$$m_{k+1} = Pm_k^*$$
$$C_{k+1} = PC_k P^t + C_w$$

- **Smoothing step:**
  a posteriori smoothing of the calculated series, based on Gaussian hypothesis for the correlation time

$$m_k^s = m_k^* + G_k(m_{k+1}^s - m_{k+1})$$
$$C_k^s = C_k^* - G_k(C_{k+1} - C_{k+1}^s)G_k^t$$
$$G_k = C_k^* P^t C_{k+1}^{-1}$$

Description of the hourly models

- **Spatial power spectra**

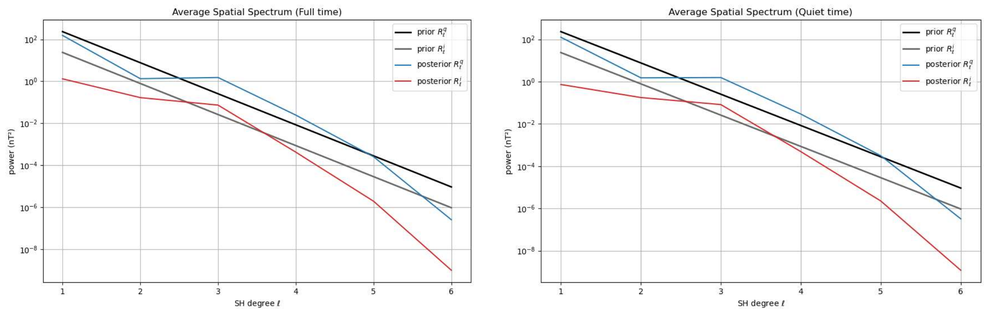

Figure 5: Average Power spectrum of hourly Spherical Harmonic (SH) Gauss coefficient as a function of SH degree over 26 years for all geomagnetic time (Left) and for geomagnetically quiet time only (Right). The solid lines are a priori power spectrum (black for the magnetospheric field, grey for the induced field). The colored lines are posterior power spectrums (blue for the magnetospheric field, red for the induced field).

- **Temporal power spectra**

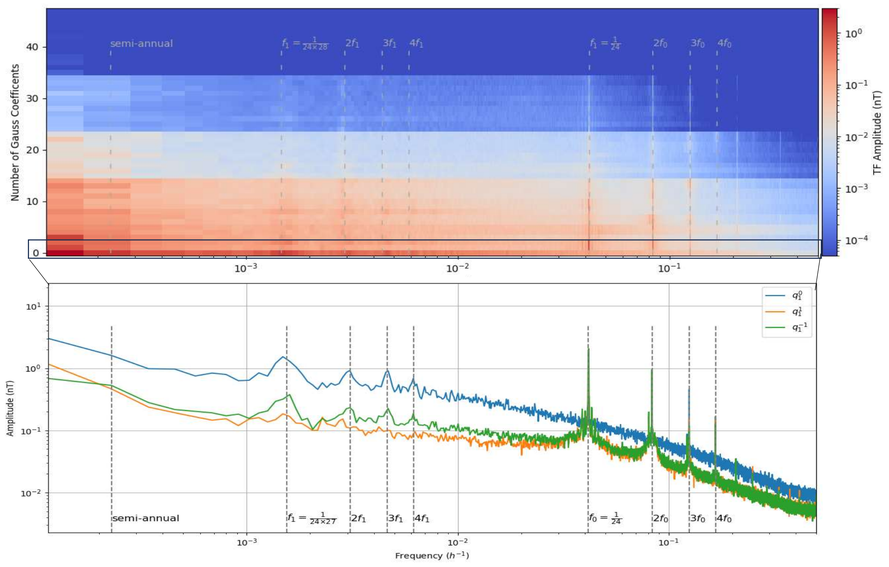

Figure 6: The temporal spectrogram analysis of magnetospheric modeling Gauss Coefficient. Top: The median temporal spectra of each Gauss coefficient (in each row) up to degree 6. Bottom: The zoom of the black box of top figure, the median temporal spectrum of the external Gauss coefficient for degree L=1. The bleu spectrum is for q10 signal, the orange for q11 and the green for q1-1. The median temporal spectrum covered periods from 2 hours to 8760 hours (one year).

- **Asymetric structure, Russel-Mcpherron effect**

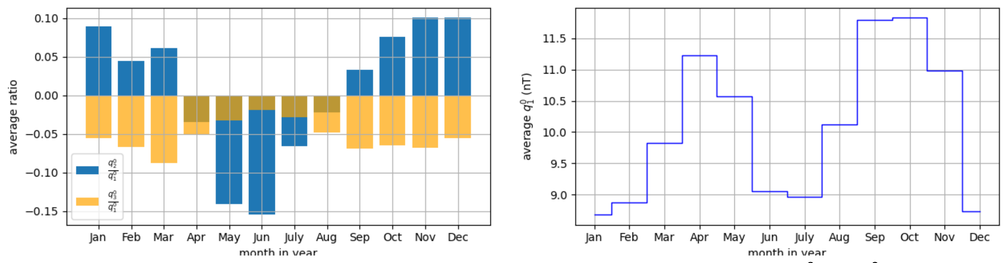

Figure 7: asymmetric structure. Left: The 26-year average of the ratio between external GC q_2^0 and q_1^0 (blue bar chart) and of the ratio between q_3^0 and q_1^0 (orange bar chart) in function of the months. Right: The 26-year average of the q_1^0 on function of the months.

- **Solar cycles**

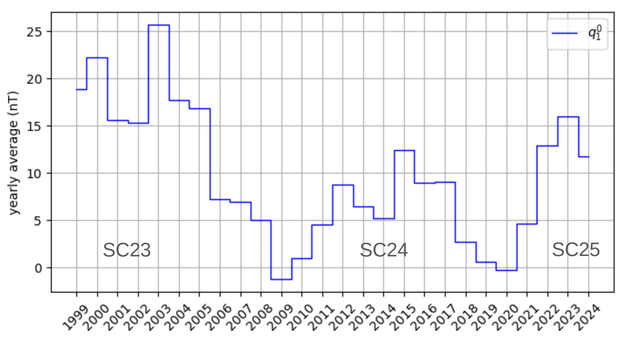

Figure 8: The distribution of q_1^0 annual averages from 1999 to 2024, which shows the variation of q_1^0 with the two solar cycles.

Assessment of the hourly models

- **Comparison with RC and Dst index**

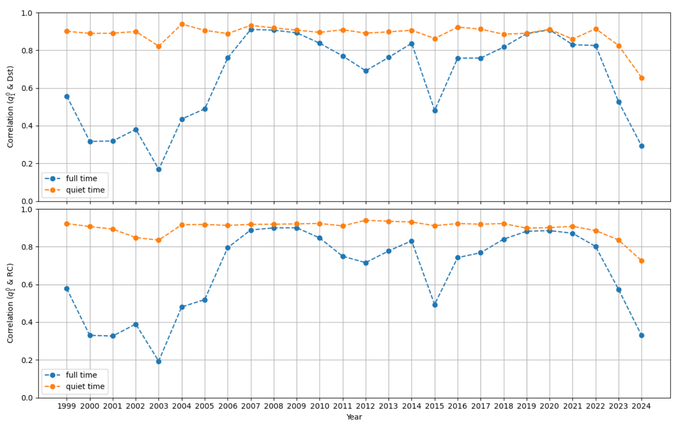

Figure 2: Annual correlation coefficient between the q_1^0 and the Dst index (top); between q_1^0 and RC index (bottom) from 1999 to 2024. The orange curve presents the correlation for geomagnetically quiet time and the blue one for all times.

	RMSE		CC		Average		
	RC^e	Est	RC^e	Est	RC^e	$-q_1^0$	Est
Full period	12.62	13.16	0.7	0.53	-11.68	-10.63	-9.19
Quiet period (-30<Dst<30 nT)	4.26	8.47	0.92	0.7	-6.68	-8.55	-5.3
Active period (|Dst|≥30 nT)	31.92	29.7	-0.17	-0.17	-42.1	-23.25	-36.4
	RC^i	Ist	RC^i	Ist	RC^i	$-i_1^0$	Ist
Full period	4.63	4.81	0.48	0.46	-0.03	-0.77	-2.94
Quiet period (-30<Dst<30 nT)	2.51	2.17	0.77	0.74	1.3	-0.5	-5.3
Active period (|Dst|≥30 nT)	10.64	12.35	-0.06	-0.19	-8.17	-2.4	-11.65

Table 1: Root-Mean-Square Errors (RMSE) in nT and Correlation Coefficient (CC) between the RC index, Dst index and minus the modeling SH Gauss coefficient (top: q_1^0, bottom: i_1^0) from 1 January 1999 to 1 August 2024.

- **Data Fitting**

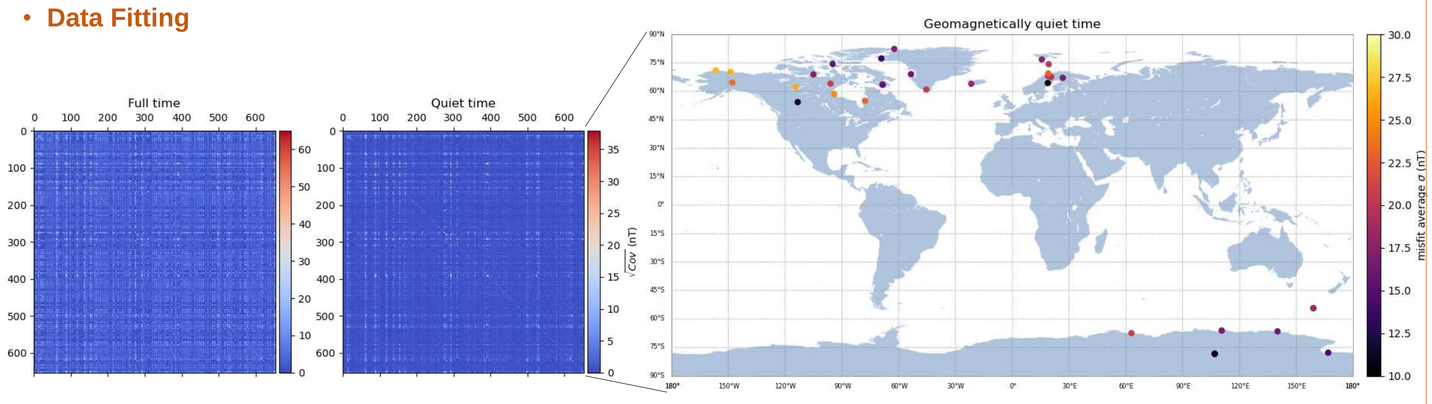

Figure 3: The covariance matrix of residuals between observatory data and modelling signal for the 218 observatory over 26 years during all geomagnetic times (Left) and quiet times (Right). The shape of the covariance matrix is (3×218,3×218).

Figure 4: The geomagnetic observatory positions are shown with 26y residual σ (diagonal elements of Fig.3: right) greater than 10nT during geomagnetically quiet time. The colorbar indicates the average σ over 3 components (x,y,z)

Future works

- Applying the methodology during the geomagnetically active periods
- Applying better statistics from theoretical or semi-empirical models in order to separate the different contributions in the magnetosphere and develop a better description of magnetospheric time variations over solar cycles

References

1. Langel R.,Sabaka T., Baldwin R., Conrad J. (1996). The near-Earth magnetic field from magnetospheric and quiet-day ionospheric sources and how it is modelled. Physics of the Earth and Planetary Interiors, 98(3-4), 235-267.
2. Finlay CC., Lesur V., Thebault Erwan, Vervelidou Foteini Morschhauser Achim, Shore R. (2017). Challenges handling magnetospheric and ionospheric signals in internal geomagnetic field modelling. Space Science Reviews 206: 157-189.
3. Kalman RE (1960). A new approach to linear filtering and prediction problems. J Basic Eng 82:35-45.
4. Holschneider M, Lesur V. Mauberberger S, Baerenzung J (2016). Correlation based modelling and separation of geomagnetic field components. J Geophys Res Solid Earth 121:3142-3160.
5. Leonie J.L. Pick, Monika Korte (2017). An annual proxy for the geomagnetic signal of magnetospheric currents on Earth based on observatory data from 1900-2010. Geophys. J. Int. 211: 1223-1236.
6. Ropp G., Lesur V., Baerenzing J., & Holschneider M. (2020), Sequential modelling of the earth's core magnetic field. Earth, Planets and Space, 72(1):1-15.
7. Stefan Maus, Hermann Luhr (2005). Signature of the quiet-time magnetospheric magnetic field and its electromagnetic induction in the rotating Earth. Geophys. J. Int. 162: 755-763.
8. Astrid Maute (2017). Thermosphere-Ionosphere-Electrodynamics General Circulation Model for the Ionospheric Connection Explorer: TIEGCM-ICON. Space Sci Rev.